Polarized optical absorption in carbon nanotubes: A symmetry-based approach

I. Milošević,* T. Vuković, S. Dmitrović, and M. Damnjanović
Faculty of Physics, University of Belgrade, P.O. Box 368, Belgrade 1101, Yugoslavia
(Received 25 October 2002; revised manuscript received 14 February 2003; published 28 April 2003)

Using density functional theory results as input data into the tight binding method for induced representations (based on the line group symmetry concept) we calculate optical conductivity tensor for single wall carbon nanotubes. Optical transition matrix elements are calculated exactly, out of completely symmetry adapted Bloch eigenfunctions. The results obtained can improve optical spectroscopy method as single-wall carbon nanotubes macroscopic sample characterization tool.

I. INTRODUCTION

Prediction of the polarization dependent optical absorption[1] in carbon nanotubes[2] (CNTs) was confirmed by optical ellipsometry[3] as well as by reflectivity measurements.[4] In addition, recent polarized Raman spectroscopy on fibers of aligned single-wall carbon nanotubes (SWCNTs), reflectance and absorption spectra and tensor invariant measurements of the Raman active modes[5] gave evidence of strongly polarized optical transitions. Recently, polarized optical absorption spectra of 4-Å-diameter tubes arrayed in channels of a zeolite single crystal has been measured and theoretically estimated on the basis of the local density function approximation.[6] Anisotropy of the dielectric function has been studied in detail in the work of Tasaki *et al.*:[7] a substantial optical rotatory power and circular dichroism as well as optical activity of the CNT ensemble have been predicted. Recently, polarized low-frequency optical spectra of SWCNT bundles, within the gradient approximation and the lowest-order isotropic model, has been calculated.[8] On the other side, optical activity[9] and anisotropy of absorption[10,11] in the isolated CNT have been inferred on the line group approach basis. Quite recently local density functional theory calculations of electro-optical properties of 4-Å carbon nanotubes have been reported.[12]

Being both individual and bulk sensitive, the optical response measurements[13–15] are, together with Raman[16] and neutron scattering and electron and x-ray diffraction, widely used as a tool for diameter and chirality distribution analysis and for a total SWCNT yield estimations in macroscopic samples. Further comprehensive theoretical study of optical transitions could considerably improve this technique.

We evaluate numerically, using the line group theoretical methods,[17] the optical conductivity tensor for individual SWCNT's of an arbitrary geometry. We use density functional tight binding (DFTB) calculations[18] as an input for the POLSym (Ref. 17) code which is based on the tight binding (TB) method for representations of the induced type[19] (electron correlations and curvature effects are included). The full line group symmetry[9] of the SWCNTs is taken into account and the $\pi \to \pi^*$ transition matrix elements of the momentum operator are, within the dipole approximation, exactly calculated out of the recently determined generalized Bloch eigenfunctions.[20] With the help of such a method the calculations are considerably simplified, enabling (computer space and time) economic evaluations of electron bands and optical absorption functions, even for highly chiral SWCNTs having a huge number of atoms within a unit cell.

Our approach goes beyond both joined density of states (JDOS) and gradient approximations to the absorption spectrum and beyond the zone-folding and the lowest-order isotropic TB model of electron dispersion. By using the full symmetry group and symmetry adapted basis we are able to calculate transition matrix elements analytically. However, the calculation procedure itself, based on a rather simple application of the quite technical Wigner-Eckart theorem extension to the inductive spaces, is beyond the scope of this paper and will be published elsewhere.[23]

In this work we calculate the polarized optical conductivity for isolated SWCNTs of diameters 0.8–1.6 nm. In addition, we carry out calculations for bundled SWCNTs with a mean diameter of 1.36 nm, assuming a Gaussian diameter distribution with $\Delta d = 0.05$ nm. We find that the chirality dependence of optical transition probabilities should not be neglected for perpendicular (to the tube axis) polarization. In other words, the JDOS approximation to the optical conductivity is not reliable in such a case. On the other side, for a parallel polarization the JDOS based results are generally in a good agreement with the more accurate calculations. Apart from the overall absorption intensity enhancement, the JDOS results differ only slightly in relative intensities of the peaks, their shapes and centers of gravity.

II. SYMMETRY AND BAND ASSIGNATION

Line groups[17] (also referred as rod or monoperiodic groups) are spatial symmetries of quasi-one-dimensional crystals (like space groups are the symmetries of the three-dimensional ones). Consequently, the geometrical symmetries of an infinitely long SWCNT form a line group. For chiral (n_1, n_2), zigzag $(n, 0)$ and arm-chair (n, n) SWCNTs ($\mathcal{C}$, $\mathcal{Z}$, and $\mathcal{A}$, for short) these are[9] $\mathbf{L}_\mathcal{C} = \mathbf{T}_q^r \mathbf{D}_n = \mathbf{L}q_p 22$, $\mathbf{L}_{\mathcal{Z}\mathcal{A}} = \mathbf{T}_{2n}^1 \mathbf{D}_{nh} = \mathbf{L}2n_n/mcm$. Here, n is the greatest common divisor of n_1 and n_2, $q = 2(n_1^2 + n_1 n_2 + n_2^2)/n\mathcal{R}$ [$\mathcal{R} = 3$ if $(n_1 - n_2)/3n$ is an integer; otherwise $\mathcal{R} = 1$], while the parameters r and p describe the helicity by more complicated functions[9] of n_1 and n_2. The general line group element is $l(t, s, u, v) = (C_q^r | na/q)^t C_n^s U^u \sigma_v^u$ where C_n^s ($s = 0, ..., n-1$) is a rotation by $2\pi s/n$ around the tube axis (z axis), Koster-Seitz symbol $(C_q^r | na/q)^t$ ($t = 0, \pm 1, ...; a$ is the translational

period of the tube) denotes a rotation by $2rt\pi/q$ around the tube axis followed by a translation along it for nat/q, while U is the rotation through π around the horizontal, x axis ($u = 0,1$). $\mathcal{Z}$ and $\mathcal{A}$ tubes have an extra symmetry: a vertical mirror reflection σ_v in the xz plane (for $\mathcal{C}$ tubes one should take $v = 0$). Note that, having both σ_v and U symmetries, $\mathcal{Z}$ and $\mathcal{A}$ tubes have the horizontal (xy) mirror plane symmetry $\sigma_h = \sigma_v U = U\sigma_v$ as well. By mapping any carbon atom by the entire set of $l(t,s,u,0)$ transformations [which are concretely defined by the wrapping indices (n_1,n_2)] one builds a corresponding tube. In other words, the SWCNT is a single-orbit system and its carbon atoms can be labeled by a triple (t,s,u): C_{tsu}, and each pair of the atoms is related by some line group transformation [for instance, $C_{tsu} = l(t,s,u,0)C_{000}$].

Since this way the symmetry completely determines the SWCNT itself, it is essential for understanding its underlying physical properties. The full symmetry group yields a complete set of quantum numbers: the z component m of the angular momentum, the linear quasimomentum k [m takes integer values from the interval $(-q/2,q/2]$, while k runs over the Brillouin zone $(-\pi/a,\pi/a]$] and the $+/-$ parities with respect to the z-reversal symmetries. For achiral tubes there are vertical mirror parities A/B as well. Recently, line group symmetry assignment of SWCNTs electronic bands has been performed and the corresponding symmetry adapted generalized Bloch eigenfunctions have been derived together with the selection rules.[20]

Electronic energies and states are calculated within the maximally adapted (to the state space structure) TB model. Namely, our approach goes beyond the conventional TB techniques[21] as we, using the full symmetry group, developed the minimal full symmetry implementing algorithm; this is essential in calculations of electro-optical properties of highly chiral tubes. It is based, technically, on the modified Wigner projectors technique (details on the method are presented in Ref. 19 and references therein). We take into account single $2p_z$ orbital $|tsu\rangle$ per carbon atom C_{tsu} as we consider enough thick tubes for curvature effects not to be strong and the optical absorption in the energy range 0–6 eV. Namely, due to the relatively small curvature of the tubes considered the hybridization effects can be neglected,[22] the states around the gap or Fermi level are essentially π or π^* derived and the $\pi \to \pi^*$ transitions give dominant response to light with the energy below 6 eV.[7] In general case (chiral tube double band degeneracy) an irreducible part of the Hamiltonian[20] $H = \Sigma\, \gamma_{tsu,t's'u'}|tsu\rangle\langle t's'u'|$ (summation is over the entire range of all the indices, i.e., further neighbor interaction and local distortions are included) is of the form

$$H_m(k) = \begin{pmatrix} h_m^0(k) & h_m^{1*}(k) \\ h_m^1(k) & h_m^0(k) \end{pmatrix}, \quad (1)$$

where

$$h_m^u(k) = \sum_{ts} \gamma_{tsu,000}\, e^{i\psi_k^m(t,s)},$$

and

$$\psi_m^k(t,s) = \frac{kan + 2\pi mr}{q}\, t + \frac{2\pi m}{n}\, s.$$

Note that, due to the non orthogonality of the basis states ($\langle tsu|t's'u'\rangle \neq 0$), $\gamma_{tsu,000} \neq \langle tsu|H|000\rangle$. However, in order to invoke the well known overlaps and Slater-Koster matrix elements,[24,18] we transform Eq. (1) by substituting $\gamma_{tsu,000}$ with $\langle tsu|H|000\rangle$ and by multiplying the matrix obtained with the square root of the metric inverse. Electronic dispersions and Bloch states are then easily calculated by solving the eigenproblem: To each m there corresponds a pair of bands $\epsilon_m^{\pm}(k)$ nearly symmetric with respect to the Fermi level. As the local curvature is taken into account a secondary gap opens up in case of primary metallic $\mathcal{Z}$ and $\mathcal{C}$ tubes. For the same reason the Fermi level crossing point k_F of the $\mathcal{A}$ bands shifts slightly from $2\pi/(3a)$ (lowest order isotropic model value) towards left.[25]

Let $|km\rangle$ denote a symmetry adapted Bloch state propagating in the z direction with quasi-momentum k and an angular momentum component m. As the two-fold horizontal axis U connects $|km\rangle$ and $|-k,-m\rangle$ [implying $\epsilon_m(k) = \epsilon_{-m}(-k)$] we can restrict our considerations to the ID (irreducible domain) $[0,\pi/a]$ throughout which the degeneracy of the $\mathcal{C}$ tube sub-bands is double. The $\mathcal{A}$ and $\mathcal{Z}$ tubes have additional vertical mirror symmetry σ_v which maps $|km\rangle$ to $|k,-m\rangle$ and $|-k,-m\rangle$ to $|-k,m\rangle$. Consequently, the degeneracy is fourfold. For $m = 0$ and $m = n$ the bands remain double-degenerate on the account of the well defined σ_v parity. These bands are σ_v invariant in the $\mathcal{Z}$ configuration (there are four of them) while in the $\mathcal{A}$ case just one pair is of the A type (σ_v invariant) and the other one of the B type (changes sign under σ_v transformation).

At most eight (and at least four) $\mathcal{C}$ tube edge states have the z-reversal $(+/-)$ parity: at $k = 0$ for $m = 0$, $q/2$ and at $k = \pi/a$ for $m = -p/2$, $(q-p)/2$ (for p even only[9]). Since the above listed m-values are equivalent to the ones of the opposite sign, by the U symmetry imposed energy relation becomes $\epsilon_m(k) = \epsilon_m(-k)$ implying van Hove singularities in the electron DOS at the ID edges that are labeled by these specific angular momentum quantum numbers. Due to the extra horizontal mirror symmetry σ_h all the $k = 0$ states of the achiral tubes are $+/-$ labeled. For the $\mathcal{A}$ tubes all of them are $+$ while for the $\mathcal{Z}$ ones there are equal number of odd and even states: a $+/-$ pair for each m. This additional symmetry imposes the condition $\epsilon_m(k) = \epsilon_m(-k)$, i.e., the zero slope at $k = 0$ for every m and at $k = \pi/a$ for $m = n/2$.

III. OPTICAL CONDUCTIVITY

In the relaxation-time approximation, the interband contribution (at absolute zero temperature) to the real part of the optical conductivity tensor is (here we give only the expression for the diagonal elements as, due to the tubes symmetry, the non-diagonal ones vanish[9]):

$$\mathrm{Re}\,\sigma_{jj} = \frac{C}{\omega}\sum |\langle k_f m_f \Pi_f|\nabla_j|k_i m_i \Pi_i\rangle|^2\,\delta(\Delta\epsilon - \hbar\omega), \quad (2)$$

where $C = 2\pi e^2 \hbar^2 / m_e^2$, $\Delta\epsilon = \epsilon_f - \epsilon_i$ is the energy absorbed, j denotes the direction of the electric field applied, and the subscripts i and f refer to the initial and the final state respectively and the summation runs over quantum numbers k_i, m_i, Π_i, k_f, m_f, Π_f (Π represents parities). As only two tensor components are independent[9] we introduce the following notation: $\sigma_{zz} = \sigma_\parallel$, $\sigma_{xx} = \sigma_{yy} = \sigma_\perp$. The form of the expression used is convenient for the selection rules application. For any orientation of the electric field, the wave vector of the Bloch electron remains essentially unchanged in the optical transition: the crystal momentum conservation law reads $\Delta k = 0$.

Operator $\nabla_\parallel$ is reversed upon the U transformation and invariant under all the others ($_0A_0^-$ tensor of the group $\mathbf{L}_\mathcal{C}$ and $\mathbf{L}_{\mathcal{Z,A}}$). As for ∇_x and ∇_y, it is convenient to switch to the momentum standard components $\nabla_\pm = \nabla_x \pm i\nabla_y$ as these carry the two-dimensional space of the IR $_0E_1$ for $\mathcal{C}$ and $_0E_1^+$ for the achiral tubes. The dipole optical transition selection rules are now easy to deduce.

The quasiangular momentum m selection rules depend on the direction of the perturbing electric vector: if it is parallel to the tube axis ($\parallel$ polarization) the rule imposes $\Delta m = 0$ while if it is orthogonal onto the z axis ($\perp$ polarization) Δm should be 1 (left circular polarization) or -1 (right circular polarization) in order the dipole optical transition to take place.

As for the parities (if defined) the one with respect to σ_v is to be preserved while the one with respect to U axis or to σ_h is to be reversed in the case of $\parallel$ polarization. For $\perp$ polarization it is *vice versa* concerning the σ_h parity while no restriction is imposed onto the σ_v parity.

Taking into account the selection rules and substituting Σ_k by $1/\pi \int_k dk$ in Eq. (2) one finds

$$\mathrm{Re}\,\sigma_\parallel = \frac{C}{\omega}\sum_m \int_0^\pi \mathrm{Im}\left[\frac{|\langle km;+|\nabla_\parallel|km;-\rangle|^2}{\epsilon_m^+(k) - \epsilon_m^-(k) - \hbar\omega - i\eta}\right]dk, \quad (3)$$

where $|km;\pm\rangle$ represent the Bloch orbitals above and below the Fermi level respectively, while $\eta = 0.04$ eV is a phenomenological broadening that suppresses height of the resonant peaks. Analogously, starting from Eq. (2) it is straightforward to obtain the relation for the perpendicularly polarized field:

$$\mathrm{Re}\,\sigma_\perp = \frac{C}{\omega}\sum_m \int_0^\pi \mathrm{Im}\left[\frac{|\langle k,m+1;+|\nabla_+|k_m;-\rangle|^2}{\epsilon_{m+1}^+(k) - \epsilon_m^-(k) - \hbar\omega - i\eta}\right.$$
$$\left. + \frac{|\langle k,m-1;+|\nabla_-|km;-\rangle|^2}{\epsilon_{m-1}^+(k) - \epsilon_m^-(k) - \hbar\omega - i\eta}\right]dk. \quad (4)$$

Note that for $\mathcal{A}$ tubes $\parallel$ transitions for $m = 0$, n are to be excluded as doubly degenerate electronic bands have different vertical mirror symmetry. Concerning the $+/-$ parities, they are implicitly taken into account as symmetry adapted state functions are used. Namely, in spite of the systematic strong van Hove singularities, the $\parallel$ transitions between the states with nonvanishing k (but close to $k = 0$) are highly suppressed. This is due to the continuity principle since the
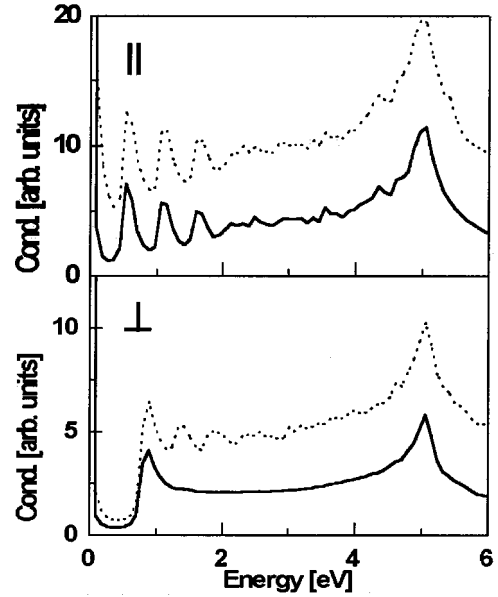

FIG. 1. Components of the optical conductivity tensor (solid lines) and the JDOS approximation to them (dotted lines) for the (10,10) bundle. Intensity of the optical conductivity of the bundle is normalized to a single tube.

transitions are forbidden at $k = 0$ by the z-reversal symmetry. As for the $\perp$ transitions, the parity selection rules are of no importance for the $\mathcal{A}$ tubes.

By contrast, for $\mathcal{Z}$ tubes the $\parallel$ transitions are not affected by the parities while the $\perp$ transitions are almost entirely suppressed by them. For this type of tubes there are no DOS peaks out of $k = 0$ vicinity while the z-reversal symmetry forbids the $\perp$ absorption at $k = 0$. Owing to the matrix elements' continuity, the corresponding transition probabilities are small and the $\perp$ optical spectra features are highly suppressed despite the strong van Hove singularities.

Concerning the $\mathcal{C}$ tubes, although the parities practically do not influence the optical absorption, we find that the transition probabilities are strongly helicity dependent: the results obtained considerably differ from the JDOS-approximated ones.

IV. ABSORPTION SPECTRA FEATURES

A typical $\parallel$ polarized absorption spectrum of the bundled SWCNTs [29 tubes comprising the (10,10) bundle: a Gaussian distribution centered at $d = 1.36$ nm with $\Delta d = 0.05$ nm] is depicted in the upper panel of Fig. 1. Note that each tube in the bundle is weighted with a Gaussian factor, i.e., the absorption intensity is normalized to a single tube. The first two peaks at 0.55 and 1.1 eV are the well-known semiconducting tubes response that scale inverse with the tube diameter. The third feature, at 1.65 eV, scaling up also with $1/d$, comes from (metallic) $\mathcal{A}$ tubes and from primary metallic $\mathcal{Z}$ and $\mathcal{C}$ ones. In Figs. 2 and 3 a diameter dependence of the transition energies of the two lowest inter-band optical transitions (ϵ_1^{sc} and ϵ_2^{sc}) in the semi-conducting tubes is presented. The linear fit is made over all the SWCNTs within the presented diameter interval although the peak positions for the zigzag tubes are particularly highlighted. While all
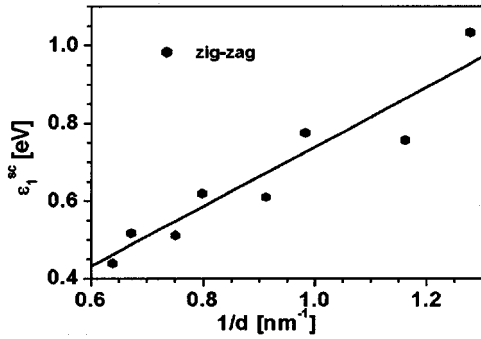
FIG. 2. Diameter dependence of the first ∥ polarized optical transition ϵ_1^{sc} in semiconducting SWCNTs. The lines fit the data obtained for all the tubes in a given diameter range, while the dots represent the zigzag tubes only.

FIG. 4. Diameter dependence of the lowest interband transition ϵ^m in the (primary) metallic SWCNTs. Linear fit is made for all the (primary) metallic tubes in a given diameter range while the dots and represent the zigzag and armchair tubes only.

the values ϵ_2^{sc} for the zigzag tubes fall into the fitted line, the ϵ_1^{sc} values show a dispersing behavior: those satisfying $n - n' = 1$ (mod3) are above, while the ones with $n - n' = -1$ (mod3) are below it. Concerning tubes that mostly comprise the bundle here considered, i.e. the ones with the diameter $d = 1.36$ nm, only the position of the first peak in the spectrum is slightly upshifted relative to the corresponding one in the spectrum of the bundle: for the tube (12,8) it shows up at 0.6 eV.

The calculations, when compared to the measurements of Kataura *et al.*[26] (on pure SWCNTs produced by using the catalyst NiY at the temperature of 1200 °C with the same mean diameter) agree nicely regarding the third peak position (1.65 eV versus 1.7 eV, i.e., 3% downshift), while the calculated first two transition energies are 13% and 9% downshifted, respectively, relative to the measured values. This may be attributed to the intertube interaction within a bundle and other inevitable discrepancies between the idealized model of an infinite isolated SWCNT and the real measurements on a macroscopic SWCNT sample. Also, in this paper we have used a minimal basis set of only one p orbital per carbon atom. Finally, the Coulomb interaction between the π-band electrons has been included only through the mean field theory (DFTB input to the TB procedure). According to the recent theoretical and experimental analysis[27] such an interaction could cause an upshift of the transition energies, in particular of the lowest ones.
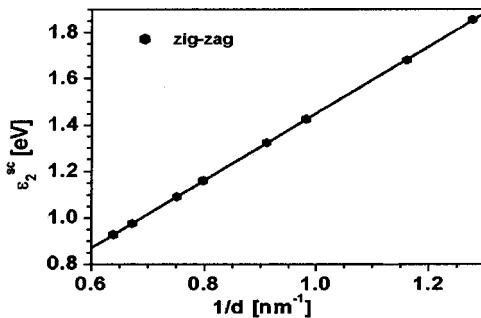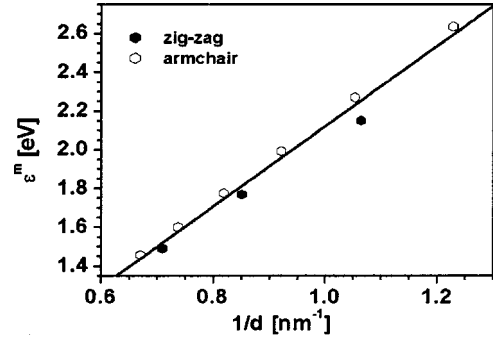
The inverse diameter dependence of the position ϵ^m of the third peak (coming from the lowest optical inter-band transition in $\mathcal{A}$ tubes and primary metallic $\mathcal{Z}$ and $\mathcal{C}$ ones) is given in Fig. 4. Here also the fit is made over all the data though only achiral tubes peak positions are specially marked.

The collective excitation of the π-electron system (at zero-momentum transfer) in the tubes with the (10,10)-bundle typical diameters, we find (for both polarizations) at 5 eV (Fig. 1), which is in a good agreement with the electron-energy-loss spectroscopy measurements[28] and other theoretical predictions.[29] Considerable anisotropy is evident although the excitation is well pronounced for the $\perp$ polarized electric field as well. In the range between the low-energy inter-band transitions (ϵ_2^{sc} or ϵ^m) and the π-plasmon excitation energy few interband optical absorption features appear. As they are highly sensitive to the helicity of the particular tube (regarding the peak positions and absorption intensities), after averaging over a bundle they result in rather broad and weakly pronounced peaks. Their wrapping-angle sensitiveness is illustrated in Fig. 5 by tubes with diameter $d = 1.36$ nm.

The main features of the $\perp$ polarized optical spectra (of the same SWCNT bundle) are given in Fig. 1 lower panel. These are responses from all the types of the tubes within the bundle apart from the tubes (15,3), (16,4), (15,5), (14,5),
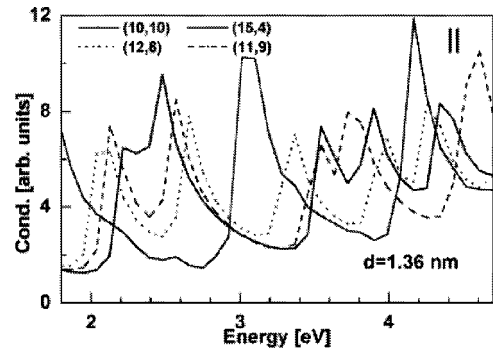

FIG. 3. Diameter dependence of the second ∥ polarized optical transition ϵ_2^{sc}, in semiconducting SWCNTs. The lines fit the data obtained for all the tubes in a given diameter range, while the dots represent the zigzag tubes only.

FIG. 5. Highly helicity sensitive ∥ polarized absorption spectra features (in the energy region between the well pronounced low-energy peaks and the onset of the π plasmon) for SWCNTs (10,10), (15,4), (12,8), and (11,9) having the same diameter $d = 1.36$ nm but different wrapping angles.
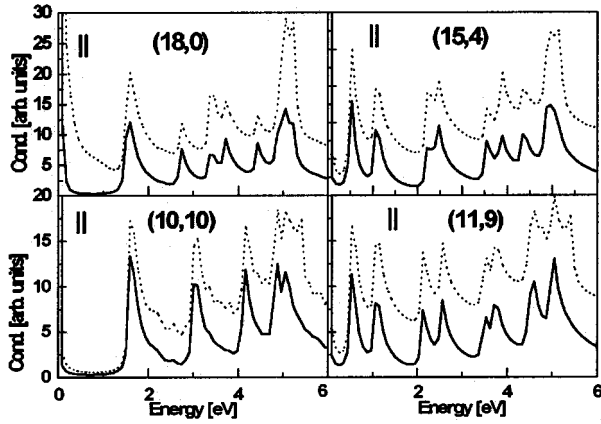
FIG. 6. ∥ component of the optical conductivity (bold line) and the JDOS approximation to it (dotted line) for SWCNTs (18,0), (15,4), (10,10), and (11,9).

(13,5), (14,6), and (13,7) which are practically transparent throughout the entire range for such a polarization of the electric field.

We now turn to the inspection of the differences between the results here presented and the widely used JDOS-approximated ones based on the lowest-order isotropic TB model. For ∥ polarization the JDOS only based results are, aside from the overall absorption intensity enhancement and slight differences regarding peak positions, their relative intensities and shapes, in reasonably good agreement with more accurate calculations (Fig. 6). These differences seem to be more pronounced for the tubes with small wrapping angle ($\mathcal{Z}$ tubes and tubes close to the $\mathcal{Z}$ direction) but can be scarcely noticed when averaged over a bundle. This is illustrated in the upper panel of Fig. 1. On the contrary, in case of the ⊥ polarization, the JDOS approximation leads to the incorrect predictions. As is evident from the calculated spectra for the (10,10)-bundle (Fig. 1, lower panel), many of the absorption peaks resulting from the JDOS approximation to the ⊥ component of the optical conductivity tensor, do not appear in the more accurately calculated optical spectrum. For isolated SWCNTs these discrepancies are even more noticeable. For the sake of comparison see Fig. 7.
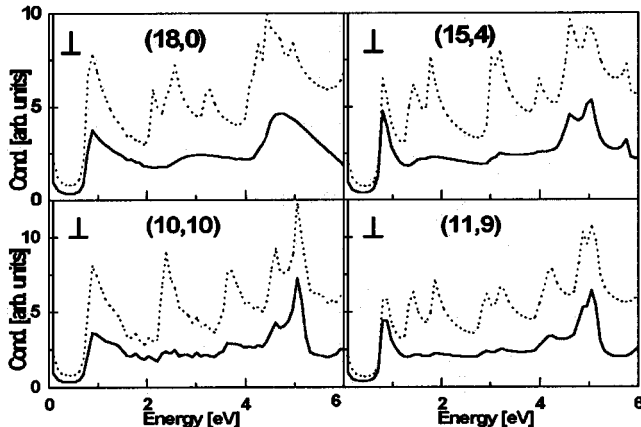

FIG. 7. ⊥ component of the optical conductivity (bold line) and the JDOS approximation to it (dotted line) for SWCNTs (18,0), (15,4), (10,10), and (11,9).

V. DISCUSSION

Using the line group symmetry we have theoretically investigated the polarized optical conductivity of the isolated SWCNTs with diameters between 0.8 and 1.6 nm and of the standard SWCNT bundle (mean diameter 1.36 nm and distribution width 0.05 nm), without taking into account the inter-tube interaction. The electron band structure is calculated by the TB method for induced representations[19] while the optical transition matrix elements are evaluated (in the dipole approximation) out of fully symmetry adapted generalized Bloch eigenstates.[20] As input data, the results of the DFTB calculations[18] are used. Due to the mathematical background applied here (which requires ideal geometrical structure of the tubes and neglects the end effects), the numerical evaluations proved to be very efficient.

Unlike the widely used optical absorption simulations dealing with the constant matrix elements[10,15,16] in the procedure applied here the transition probabilities are thoroughly calculated. Our approach also refines the isotropic TB electronic dispersion evaluations that include the so called "π-π overlap integral" γ_0 as a fitting parameter. There is a wide agreement[30] that with γ_0 between 2.9 and 3 eV the calculations very well match the measured values except for the very thin tubes where the refitting is required. Surprisingly enough, adoption of the value $\gamma_0 = 2.55$ eV, which is quite close to the TB calculated result for the graphene plane, fits the best.[16] Namely, as recently has been pointed out by Kuzmany et al.,[16] one would rather expect γ_0 to increase with the curvature.

According to the detailed quantum mechanical considerations that we have applied here the overlaps $\langle tsu|t's'u'\rangle$ of the neighboring atomic orbitals $|tsu\rangle$ and $|t's'u'\rangle$ increase with the curvature. On the other side, the notion of the "overlap integral γ_0" is not applicable to the approach of ours. However, in somewhat vague terms it can be taken that γ_0 corresponds to the Hamiltonian matrix ($\langle tsu|H|t's'u'\rangle$) divided by the square root of the metric (i.e. matrix which elements are the overlaps). As the elements $\langle tsu|t's'u'\rangle$ increase with the curvature, it is reasonable to expect the "overlap integral γ_0" to diminish simultaneously.

The results obtained reinforce the JDOS approximation to the optical conductivity for ∥ polarized electric field but lead to quite different conclusions as far as the ⊥ component of the conductivity tensor is considered. The discrepancies are most prominent for thin $\mathcal{Z}$ tubes but also quite substantial even when the JDOS-only-based results are averaged over a bundle. We explain this by the parity selection rules influence to the transition probabilities, elucidating that the JDOS approximation is conceptually incompatible with the horizontal mirror parity selection rules for dipole absorption processes in the achiral SWCNTs. Namely, although very little weight is associated with the horizontal mirror parity states (as only for a finite number of the high symmetry states this parity is well defined) due to the continuity principle (which cannot be included within the JDOS approximation), if the transition is not permitted at $k = 0$ the transitions between the nearby states with general but non vanishing k are not very likely to occur. As all the bands of the achiral tubes are zero

sloped at $k=0$, this means that the JDOS approximation[10] to the optical absorption spectrum of the achiral CNT cannot be entirely reliable, especially not for the $\mathcal{Z}$ tubes as all their DOS van Hove singularities show up in the $k=0$ vicinity. In general, the horizontal mirror symmetry suppresses a vast number (all but two) of the perpendicularly polarized optical transitions in the $\mathcal{Z}$ tubes and all the parallel transitions close to $k=0$ in the $\mathcal{A}$ tubes. Since the number of bands enlarges with diameter and they become zero sloped over larger $k=0$ vicinity the horizontal mirror parity influence to the interband transitions is diminished for thicker tubes. In contrast, for the chiral SWCNTs the U parity does not effect the optical transitions.

The results of the comprehensive (and cumbersome) analytical and numerical study presented here could improve the polarized optical spectroscopy method as a characterization tool of the macroscopic SWCNT samples by making it more accurate and reliable.

Note added in proof: Our attention was recently drawn to a paper on a similar theme.[31]

ACKNOWLEDGMENTS

---

*Electronic address: ivag@afrodita.rcub.bg.ac.yu; URL: http://www.ff.bg.ac.yu/qmf/qsg_e.htm

[1] H. Ajiki and T. Ando, Physica B **201**, 349 (1994).

[2] S. Iijima, Nature (London) **354**, 56 (1991); A. Thess, R. Lee, P. Nikolaev, H. Dai, P. Petit, J. Robert, C. H. Xu, Y. H. Lee, S. G. Kim, A. G. Rinzler, D. T. Colbert, G. E. Scuseria, D. Tomanek, J. E. Fischer, and R. E. Smally, Science **273**, 483 (1996); C. Journet, W. K. Maser, P. Bernier and A. Loiseau, Nature (London) **388**, 756 (1997).

[3] W. A. de Heer, W. S. Bacsa, A. Chatelain, T. Gerfin, R. Humphrey-Baker, L. Forro, and D. Ugarte, Science **268**, 845 (1995).

[4] F. Bommeli, L. Degioergi, P. Wachter, W. S. Bacsa, W. A. de Heer, and L. Forro, Solid State Commun. **99**, 513 (1996).

[5] H. H. Gommans, J. W. Alldredge, H. Tashiro, J. Park, J. Magnuson, and A. G. Rinzler, J. Appl. Phys. **88**, 2509 (2000); J. Hwang, H. H. Gommans, A. Ugawa, H. Tashiro, R. Haggenmueller, K. I. Winey, J. E. Fischer, D. B. Tanner, and A. G. Rinzler, Phys. Rev. B **62**, R13310 (2000); S. Reich, C. Thomsen, G. S. Duesberg, and S. Roth, *ibid.* **63**, 041401(R) (2001).

[6] Z. M. Li, Z. K. Tang, H. J. Liu, N. Wang, C. T. Chan, R. Saito, S. Okada, G. D. Li, J. S. Chen, N. Nagasawa, and S. Tsuda, Phys. Rev. Lett. **87**, 127401 (2001).

[7] S. Tasaki, K. Maekawa, and T. Yamabe, Phys. Rev. B **57**, 9301 (1998).

[8] M. F. Lin, Phys. Rev. B **62**, 13 153 (2000).

[9] M. Damnjanović, I. Milošević, T. Vuković, and R. Sredanović, Phys. Rev. B **60**, 2728 (1999); J. Phys. A **32**, 4097 (1999).

[10] I. Božović, N. Božović, and M. Damnjanović, Phys. Rev. B **62**, 6971 (2000).

[11] I. Milošević, T. Vuković, S. Dmitrović, and M. Damnjanović, Physica E (Amsterdam) **12**, 745 (2002).

[12] H. J. Liu and C. T. Chan, Phys. Rev. B **66**, 115416 (2002); M. Machón, S. Reich, C. Thomsen, D. Sánchez-Portal, and P. Ordejón, Phys. Rev. B **66**, 155410 (2002).

[13] O. Jost, A. A. Gorbunov, W. Pompe, T. Pichler, R. Friedlein, M. Knupfer, M. Reibold, H.-D. Bauer, L. Dunsch, M. S. Golden, and J. Fink, Appl. Phys. Lett. **75**, 2217 (1999).

[14] S. Kazaoui, N. Minami, R. Jacquemin, H. Kataura, and Y. Achiba, Phys. Rev. B **60**, 13 339 (1999).

[15] X. Liu, T. Pichler, M. Knupfer, M. S. Golden, J. Fink, H. Kataura, and Y. Achiba, Phys. Rev. B **66**, 045411 (2002).

[16] H. Kuzmany, W. Plank, M. Hulman, Ch. Kramberger, A. Grüneis, Th. Pichler, H. Peterlik, H. Kataura, and Y. Achiba, Eur. Phys. J. B **22**, 307 (2001).

[17] I. Milošević, A. Damjanović, and M. Damnjanović, in *Quantum Mechanical Simulation Methods in Studying Biological Systems*, edited by D. Bicout and M. Field (Springer-Verlag, Berlin, 1996) Chap. XIV.

[18] D. Porezag, Th. Fraunheim, Th. Kohler, G. Seifert, and R. Kaschner, Phys. Rev. B **51**, 12 947 (1995).

[19] M. Damnjanović, T. Vuković, and I. Milošević, J. Phys. A **33**, 6561 (2000).

[20] T. Vuković, I. Milošević and M. Damnjanović, Phys. Rev. B **65**, 045418 (2002).

[21] W. A. Harrison, *Electronic Structure and the Properties of Solids* (Freemen, San Francisco, 1980).

[22] X. Blase, L. X. Benedict, E. L. Shirley, and S. G. Louie, Phys. Rev. Lett. **72**, 1878 (1994).

[23] I. Milošević, T. Vuković, T. Marinković, and M. Damnjanović, in *Proceedings of the Wigner Centennial Conference, Pécs*, edited by A. Gábris and M. Koniorczyk (2003).

[24] J. C. Slater and G. F. Koster, Phys. Rev. B **94**, 1498 (1954); R. R. Sharma, *ibid.* **19**, 2813 (1979); H. Eschrig, Phys. Status Solidi B **96**, 329 (1979).

[25] M. Damnjanović, T. Vuković, and I. Milošević, Solid State Commun. **116**, 265 (2000).

[26] H. Kataura, Y. Kumazawa, Y. Maniwa, I. Umezu, S. Suzuki, Y. Ohtsuka, and Y. Achiba, Synth. Met. **103**, 2555 (1999).

[27] T. Ando, J. Phys. Soc. Jpn. **66**, 1066 (1997); M. Ichida, S. Mizuno, Y. Tani, Y. Saito, and A. Nakamura, *ibid.* **68**, 3131 (1999).

[28] R. Kuzuo, M. Terauchi, M. Tanaka, and Y. Saito, Jpn. J. Appl. Phys. **33**, L1316 (1994).

[29] A. A. Lucas, L. Henrard, and Ph. Lambin, Phys. Rev. B **49**, 2888 (1994); M. F. Lin, D. S. Chuu, C. S. Huang, Y. K. Lin, and K. W.-K. Shung, *ibid.* **53**, 15 493 (1996).

[30] M. A. Pimenta, A. Marucci, S. A. Empedocles, M. G. Bawendi, E. B. Hanlon, A. M. Rao, P. C. Eklund, R. E. Smalley, G. Dresselhaus, and M. S. Dresselhaus, Phys. Rev. B **58**, R16016 (1998); M. Milnera, J. Kürti, M. Hulman, and H. Kuzmany, Phys. Rev. Lett. **84**, 1324 (2000); P. M. Rafailov, H. Jantoljak, and C. Thomsen, Phys. Rev. B **61**, 16 179 (2000).

[31] A. Grüneis, R. Saito, Ge. G. Samsonidze, T. Kimura, M. A. Pimenta, A. Jorio, A. G. Souza Filho, G. Dresselhaus, and M. S. Dresselhaus, Phys. Rev. B **67**, 165402 (2003).